Supporting online material for

Photodegradable hydrogels for dynamic tuning of physical and chemical properties

April M. Kloxin, Andrea M. Kasko, Chelsea N. Salinas, and Kristi S. Anseth*

*Author to whom correspondence should be addressed (E-Mail: Kristi.Anseth@colorado.edu)

This PDF file includes:

Supporting online materials

Materials and methods

Materials

Poly(ethylene glycol)-*bis*-amine (PEGdiamine, M_n ~ 3400 g/mol) was purchased from Laysan Bio, Inc (Arab, AL). Poly(ethylene glycol) (PEG) monoacrylate (PEGA, M_n ~ 375 g/mol), tetraethylmethylene diamine (TEMED), anhydrous dichloromethane (DCM), acryloyl chloride (AC), and triethylamine (TEA) were purchased from Sigma-Aldrich (St. Louis, MO). Diisopropylethylamine (DIEA), 2-(1H-benzotriazole-1-yl)-1,1,3,3-tetramethyluronium hexafluorophosphate (HBTU), 1-hydroxybenzotriazole (HOBt), and amino acids (glycine, aragine, aspartic acid, serine, and lysine) were purchased from Anaspec (San Jose, CA). 5(6)-carboxyfluorescein (carboxyfluorescein) and Rink amide resin (100-200 mesh) were purchased from EMD Biosciences (San Diego, CA). Methacryloxyethyl thiocarbamoyl rhodamine B (rhodamine methacrylate) was purchased from Polysciences, Inc (Warrington, PA). N-methylpyrrolidone (NMP) and all peptide synthesizer reagents were purchased from Applied Biosystems (Foster City, CA). Fibronectin was purchased from BD Biosciences (San Jose, CA). Cell media components were purchased from Invitrogen (Carlsbad, CA). Mouse anti-CD105 was purchased from BioVendor (Candler, NC); rabbit anti-collagen type II and mouse anti-integrin $\alpha_v\beta_3$ were purchased from Abcam (Cambridge, MA); and goat anti-mouse IgG AlexaFluor 488 and goat anti-rabbit IgG AlexaFluor594 were purchased from Invitrogen (Carlsbad, CA). All other chemicals and organic solvents were purchased from Fisher Scientific and used as received. Deionized (DI) water was purified by reverse osmosis

and filtration to 18 MΩ-cm (Barnstead NANOpure II).

Synthesis of photolabile moiety

The photolabile molecule, ethyl 4-(4-(1-hydroxyethyl)-2-methoxy-5-nitrophenoxy)butanoic acid was prepared based on the synthetic protocols of similar molecules in the literature (*S1, S2*). Briefly, in an Ar-purged flask with stir bar, acetovanillone and ethyl 4-bromobutyrate were dissolved in dimethyl formamide, and excess potassium carbonate was added. The reaction mixture was stirred overnight, precipitated in water, and filtered. The alkylated powder product was subsequently nitrated with nitric acid at 0^oC for 1 h and at room temperature for 1 h, carefully monitoring the temperature ($\leq 30^oC$). The product was precipitated in water, filtered, recrystallized from ethanol, and dried under vacuum overnight. The nitrated powder product in ethanol was reduced with excess sodium borohydride at 38^oC. The reaction was stirred overnight, precipitated in water, filtered, and dried under vacuum. The alcohol powder product was finely ground and reacted with aqueous trifluoroacetic acid (TFA) at 90^oC overnight. Additional TFA was added until reaction completion was verified by thin layer chromatography (10:1, methylene chloride: acetone). The reaction mixture was cooled, filtered, washed with chilled water, and dried under vacuum overnight. Sample purity was verified by proton nuclear magnetic resonance (^{1}H NMR, Varian Inova 500 NMR Spectrometer, 11.74 Tesla field). ^{1}H NMR ($(CD_3)_2SO$): δ=12.2 (s, $CH_2CO_2\mathbf{H}$), δ= 7.6 (s, Aromatic-**H**), δ=7.4 (s, Aromatic-**H**), δ=5.5 (s, Aromatic-CHO**H**), δ=5.3 (m, Aromatic-C**H**(CH_3)OH), δ=4.1 (t, Aromatic-O$C\mathbf{H_2}CH_2CH_2CO_2H$),

δ=3.9 (s, Aromatic-OC**H$_3$**), δ=2.4 (t, Aromatic-OCH$_2$CH$_2$C**H$_2$**CO$_2$H), δ=2.0 (m, Aromatic-OCH$_2$C**H$_2$**CH$_2$CO$_2$H), and δ=1.4 (d, Aromatic-CHC**H$_3$**).

Synthesis of photodegradable monomer

The photolabile precursor (0.01 mol) was suspended in anhydrous DCM (1.4 mol) and stirred in a flask purged with Ar. TEA (0.03 mol) was added, and AC (0.025 mol) in anhydrous DCM (0.3 mol) was added dropwise at 0^{o}C. The reaction was stirred at room temperature overnight and subsequently washed with sodium bicarbonate (5 w/v % aq.), dilute hydrochloric acid (1 v/v % aq.), and DI water. The solvent was evaporated, and the liquid product was dissolved in an acetone:water mixture (50:50). This reaction mixture was stirred overnight at room temperature, filtered to remove any insoluble impurities, and extracted with DCM to recover the liquid acrylated monomer. The extracted product in DCM was sequentially washed with dilute hydrochloric acid (1 v/v % aq.) and DI water, dried over magnesium sulfate, and evaporated to dryness (photodegradable monomer, PDA, 70% yield). ^{1}H NMR ((CD$_3$)$_2$SO): δ=12.2 (s, CH$_2$CO$_2$**H**), δ=7.6 (s, Aromatic-**H**), δ=7.2 (s, Aromatic-**H**), δ=6.4, 6.05 (d, d, OC(=O)CH=C**H$_2$**), δ=6.35 (m, Aromatic-C**H**(CH$_3$)OC(=O)CH=CH$_2$), δ=6.25 (m, OC(=O)C**H**=CH$_2$), δ=4.1 (t, Aromatic-OC**H$_2$**CH$_2$CH$_2$CO$_2$H), δ=3.9 (s, Aromatic-OC**H$_3$**), δ=2.4 (t, Aromatic-OCH$_2$CH$_2$C**H$_2$**CO$_2$H), δ=2.0 (m, Aromatic-OCH$_2$C**H$_2$**CH$_2$CO$_2$H), and δ=1.4 (d, Aromatic-CHC**H$_3$**).

Synthesis of photodegradable crosslinker (Compound 1)

The photodegradable acrylate monomer (6 mmol) was dissolved in NMP (156 mmol), stirred, and purged with Ar. The coupling agent HBTU (6.5 mmol), HOBt (6.5 mmol), and DIEA (11.8 mmol) were added and stirred for 5 mins upon which PEGdiamine (0.6 mmol) in NMP (104 mmol) was added. The reaction mixture was intermittently vortexed and heated until complete dissolution of all reactants. The reaction was stirred overnight, precipitated in diethyl ether at 0^{o}C, and centrifuged. The precipitated product was washed with ether and centrifuged two additional times. The macromer product was subsequently dried under vacuum, redissolved in DI water, centrifuged to remove insoluble impurities, dialyzed (SpectraPor 7, CO 1000 g/mol), and freeze dried to achieve greater than 85% modification of PEG with the photodegradable acrylate monomer (photodegradable crosslinker, Compound 1, 85% yield). ^{1}H NMR ($(CD_3)_2SO$): δ=8.0 (t, C(=O)N**H**CH_2CH_2O), δ= 7.6 (s, Aromatic-**H**), δ=7.2 (s, Aromatic-**H**), δ=6.4, 6.05 (d, d, OC(=O)CH=C**H$_2$**), δ=6.35 (m, Aromatic-C**H**(CH_3)OC(=O)CH=CH_2), δ=6.25 (m, OC(=O)C**H**=CH_2), δ=4.1 (t, Aromatic-OC**H$_2$**$CH_2CH_2CO_2H$), δ=3.9 (s, Aromatic-OC**H$_3$**), δ=3.5 (m, $[CH_2CH_2O]_n$, n~77), δ=2.75 (t, N**H$_2$**CH_2CH_2O), δ=2.4 (t, Aromatic-OCH_2CH_2C**H$_2$**CO_2H), δ=2.0 (m, Aromatic-OCH_2C**H$_2$**CH_2CO_2H), and δ=1.4 (d, Aromatic-CHC**H$_3$**).

Synthesis of photolabile peptide tether (Compound 2)

The 6-mer peptide sequence GRGDSG (glycine-aragine-glycine-aspartic acid-

serine-glycine) was synthesized on Rink amide resin using a peptide synthesizer (0.25 mmol, Applied Biosystems, model 433A). The peptide-containing resin was transferred to a glass peptide synthesis reaction vessel (10 mL, Chemglass), swelled in DCM for 30 mins, and rinsed with DCM (3x) and NMP (3x). The photodegradable acrylate monomer (1 mmol) was dissolved in NMP (<5 mL). The coupling agent HBTU (1.1 mmol), HOBt (1.1 mmol), and DIEA (2 mmol) were added to the monomer mixure and vortexed until complete dissolution. This activated-acid mixture was added to the peptide-containing resin in the reaction vessel and stirred overnight. The reaction fluid was removed, and the resin was washed with NMP and DCM. Complete reaction of the N-terminus amines on the resin-based peptide was verified with the Ninhydrin assay (*S3*). The modified peptide was cleaved from the resin in 1 hour (95% TFA, 2.5% triisopropylsilane (TIPS), and 2.5% DI H_2O). The peptide/TFA mixture was precipitated in ether and centrifuged. The peptide was washed with ether and centrifuged two additional times, dried under vacuum, and purified using high pressure liquid chromatography with an in-line UV-visible spectrophotometer (HPLC & UV-vis, Waters, C18 preparatory column, gradient 5:95 acetonitrile:H_2O to 95:5 over 70 mins, 20 mL/min, and detection wavelengths 220nm and 280nm). The purified photodegradable peptide (Compound 2) was lyophilized, and the sequence was verified using matrix-assisted laser desorption/ionization (MALDI, PerSeptive Biosystems, matrix molecule α-cyano-4-hydroxycinnamic acid).

The fluorescently-labeled photodegradable peptide was synthesized similarly. The 8-mer peptide sequence K(Mtt)GRGDSGK(Dde) (lysine-glycine-aragine-glycine-

aspartic acid-serine-glycine-lysine) was synthesized on Rink amide resin using a peptide synthesizer (0.25 mmol). The peptide-resin was transferred to a reaction vessel, swelled in DCM for 30 mins, and rinsed with DCM (3x) and NMP (3x). The N-terminus was capped with acetic anhydride over 60 mins (*S3*), the resin was rinsed with NMP and DCM, and capping was verified with the Ninhydrin assay. The K(Dde) was deprotected (2 v/v % hydrazine monohydrate in NMP, 10 mins, 2x) (*S3*), rinsed with NMP (5x) and DCM (5x), and verified with the Ninhydrin assay. Carboxyfluorescein (1 mmol) was activated with the coupling agent HBTU (1.1 mmol), HOBt (1.1 mmol), and DIEA (2 mmol) in NMP and added to peptide-resin for reaction with the deprotected pendant amine of lysine. After 2 h, the reaction fluid was removed, the resin was rinsed with NMP and DCM, and coupling was verified with the Ninhydrin assay. If coupling was incomplete, the reaction, rinsing, and verification were repeated up to 4 times. The K(Mtt) was subsequently deprotected (TFA 1.8 v/v % in DCM, 3 mins, 9x) (*S4*), rinsed with DCM (5x), and verified with the Ninhydrin assay. The PDA was attached to the deprotected pendant amine of lysine, and the resultant photodegradable fluorescently-labeled peptide was cleaved for the resin, purified, and sequence verified the same as described above for the GRGDSG peptide.

Synthesis of photodegradable PEG-based hydrogels

The redox initiator AP, base TEMED, monomer PEGA, and photodegradable crosslinker Compound 1 were each dissolved in water to give 2 M, 2 M, 40 wt%, and 20 wt% stock solutions, respectively, and each was sterile filtered. Under sterile conditions,

co-monomer solutions were prepared from these stocks to give 15 wt% total macromer in water (Compound 1:PEGA 10 mol% : 90 mol%) and 0.3 M AP. The monomer-initiator solution was vortexed as TEMED was added (0.15 M) and either quickly poured between glass slides separated by a spacer (0.5 mm) or pipetted between rheometer plates with the gap set to 0.05 mm. For 2D and 3D patterning samples, an additional fluorescent monomer was added for visualization of the resulting gel with confocal laser scanning microscopy (LSM), either an acrylated fluorescein (*S5*) or methacrylated rhodamine, and a small, asymmetric plastic shim (80 μm thick, McMaster Carr) was added during polymerization so that each sample contained an entrapped marker to maintain gel orientation during patterning and imaging. The monomers were allowed to polymerize for 5 minutes, which was determined by rheometry to give complete polymerization. From the gels created between glass slides, gel sheets were cut (10 mm x 10 mm), swelled to equilibrium in phosphate buffered saline (PBS, pH 7.4), and stored in a sterile 37^{o}C incubator until use.

Rheology and bulk degradation kinetics of photodegradable hydrogels

Optically thin gels (0.05 mm) were polymerized in situ between an 8 mm diameter flat quartz plate and a temperature-controlled Peltier flat plate (25^{o}C) attached to a photorheometer (ARES, TA). To determine the polymerization time, a dynamic time sweep was performed on polymerizing samples with strain and frequency parameters that were determined to be in the linear viscoelastic regime for both the liquid monomer solution and solid gel (γ = 10%, ω = 10 rad/s). The gel shear modulus was monitored

during polymerization until a constant value of the storage modulus (G') was observed (less than 5 minutes, data not shown). For each degradation run, monomer solutions were allowed to polymerize for 5 minutes, excess gel was removed from the exterior of the rheometer plates, the gel was surrounded by a thin bead of water to prevent dehydration, and the complex shear modulus (G*) and its two components, the storage modulus G' and viscous modulus G'', were monitored for 200 s to assure a constant initial value of G', which dominates for these elastic polymer networks (G*≈G' when G'>G'') (*S6*). The gel was subsequently degraded by exposing it continuously to UV or visible light (365 nm at 10 or 20 mW/cm^2, 405 nm at 25 mW/cm^2; Novacure, EFOS, 100W mercury arc lamp with bandpass filters, liquid-filled light guide, and collimating lens) or discontinously by shuttering the light (365 nm, 100 s with light on and 100 s with light off) while monitoring G', G'', and the torque.

A characteristic photolabile group degradation time τ was calculated from this data by fitting the following equation based on photolysis kinetics (*S7*), gel degradation kinetics (*S8*), and gel mechanical properties (*S6*)

$$\frac{G'}{G'_o} = \frac{\rho_x}{\rho_{x_o}} = \exp\left(-\frac{2t}{\tau}\right) \text{ where } \tau = \frac{N_A hc}{\phi\varepsilon\left(I_o \lambda 10^{-6}\right)},$$

where ϕ is the quantum yield of photolysis (events/photon), N_A is Avogadro's number (photons/mol), h is Planck's constant (Js), c is the speed of light (m/s), I_o is the incident light intensity (W/cm^2), ε is the molar absorptivity (Lmol^{-1}cm^{-1}), and λ is the incident light wavelength (nm). The characteristic degradation time was thus calculated for each

data set to $\frac{\rho_x}{\rho_{x_o}} \approx 0.15$ and found to scale with I_o and $\varepsilon(\lambda)$ as expected based on the kinetics of photolysis. The characteristic timescale for degradation of the photolabile moiety can thus be calculated, and degradation rates and resulting materials properties can be predicted for any light wavelength and intensity of interest.

Photolithographic erosion of photodegradable hydrogels to create post-polymerization topographic features

Equilibrium swollen optically thick fluorescently labeled photodegradable hydrogels (0.5 mm, fluorescein) in PBS were placed on a glass slide and covered with a photomask (400 μm wide black lines separated by 400 μm wide transparent lines). The masked sample was subsequently exposed to a high-intensity, broad-spectrum collimated light source to erode away the surface of the gel with a mask alignment system (320-500 nm at 40 mW/cm^2, Mask Aligner, Optical Associates Inc., Model J500) for various amounts of time (2.5 to 10 minutes) to create channels with increasing depth. The eroded surface channels and resulting topographic features were examined visually by imaging a cross-section of the gel with a confocal LSM. The features were quantitatively examined with profilometry (Stylus Profiler, Dektak 6M, force = 1 mg, radium = 12.5 mm, and range = 1 mm).

Three-dimensional patterning of photodegradable hydrogels to create 3D

To create a three-dimensional features within an initially homogeneous gel, equilibrium swollen optically thick fluorescently labeled photodegradable hydrogels (0.5 mm, rhodamine) in PBS were exposed to focused light using a single-photon confocal LSM (LSM 510, Zeiss) or two-photon confocal LSM (LSM 710, Zeiss). The photodegradable gel was submerged in PBS within a 35-mm Petri dish with a glass coverslip bottom (MatTek Corporation) and covered with a glass coverslip. Zeiss Region of Interest (ROI) software was then used to draw and subsequently scan any arbitrary shape within an x-y plane of the gel with a 405nm single-photon or 740nm two-photon laser to create a local void. These shapes subsequently were scanned in the z-direction to achieve stacked 3D voids within the gel. To demonstrate this concept, interconnected cylinders were scanned with a two-photon 740nm laser (3W laser, 20x objective NA ~ 0.75, 1 μm scan intervals over ~ 150 μm thickness, laser power = 50%, scan speed setting = 8). The resulting features were visualized with confocal LSM imaging of the fluorescent, rhodamine-labeled hydrogel, where the gel fluoresces red and the patterned void is black due to removal of the fluorescently-labeled polymer backbone and crosslinks that comprise the gel. These void features were also be imaged in brightfield. These fluorescent and brightfield raw images allow verification of the degraded region and the resulting 3D feature.

Spreading of hMSCs encapsulated in photodegradable gels

For human mesenchymal stem cell (hMSC) encapsulation experiments, adult hMSCs (Cambrex Bio Science) were plated at 5,000 cells/cm^2 in 10 cm diameter tissue culture polystyrene Petri dishes (BD Bioscience). The hMSCs were cultured in stem cell growth media (10% fetal bovine serum, 1 μg/mL amphotericin B, 50 U/mL penicillin, 50 μg/mL streptomycin, and 20 μg/mL gentamicin in Dulbecco's modified Eagle medium (DMEM) containing low-glucose, Invitrogen). The cells were grown under standard cell culture conditions (37^{o}C incubator with 5% CO_2), and media was changed twice per week. Cells were grown to confluency and passaged twice prior to encapsulation.

Adult hMSCs were encapsulated within photodegradable gels (Compound 1) at a concentration of 2x10^6 cells/mL. Monomer solutions were prepared with 100 nM fibronectin, mixed with cells, and polymerized between glass slides with a spacer for 5 min (8.2 wt% PEGdiPDA, 6.8 wt% PEGA, 100 nM fibronectin, 300 μM rhodamine-B methacrylate, 0.2 M AP, and 0.1 M TEMED in PBS, 0.25-mm thick). Gels were covalently-labeled with rhodamine B methacrylate during polymerization for visualization. Upon complete polymerization, cell-gel sheets were transferred to fresh growth media. The media was refreshed after 30 mins to remove any unreacted monomer or initiator. Media was refreshed twice per week throughout culture.

To partially degrade the hydrogel's physical structure, cell-gel constructs were flood irradiated with UV light under sterile conditions (365nm at 10 mW/cm^2 for 8 minutes per side), which based on rheometry decreases the gel crosslinking density ($\rho_x/\rho_{xo} \sim 0.4$) but does result in complete reverse gelation, releasing modified PEG and

increasing the space available to the cells. Cell spreading was observed with gel degradation, indicating that the cells responded to degradation and decreased crosslinking density of the hydrogel (Nikon TE2000S, Plan Fluor ELWD 40x NA 0.6).

Cell movement and migration within patterned photodegradable hydrogel

HT1080 fibrosarcoma cells (ATCC) were grown in Alpha MEM media (Lonza) with 10% FBS, 100 μg/mL penicillin-streptomycin, and 1 μg/mL amphotericin B. HT1080 cells were encapsulated in the photodegradable hydrogel with 100 nM fibronectin, as previously described for hMSCs, at $2x10^6$ cells/mL. Channels were degraded within these cell-gel constructs using photolithography. Samples were irradiated with UV light through a periodic photomask (365nm at 10 mW/cm^2 for 20 minutes through a photomask with 300 μm clear lines and 100 μm black lines), degrading ~ 50 μm deep channels into the gel and releasing encapsulated cells in or near the channels. Cell movement within these channels was observed over 2 days with real-time tracking in brightfield (Nikon TE2000E with motorized stage and sterile humidified 5% CO_2 chamber, Plan APO 10x NA 0.45), and the trajectories of cells of interest were followed using Metamorph. Cells were observed migrating along the degraded channels. Cells in the non-degraded sections of the gel remained immobilized.

Chondrogenic differentiation of encapsulated hMSCs with externally-triggered removal of RGDS from photolabile tether hydrogels

Adult hMSCs were thawed and expanded as previously described. hMSCs were encapsulated at a concentration of $2x10^6$ cells/mL within a non-degradable PEG-only hydrogel or a non-degradable PEG hydrogel with photolabile RGDS tether. Monomer solutions were prepared, mixed with cells, and polymerized between glass slides with a spacer for 5 min (10 wt% PEGDA or 10 wt% PEGDA with 10 mM Compound 2, 0.1 M AP, and 0.05 M TEMED in PBS, 0.3-mm thick). Experimental conditions prepared include gels (1) without RGDS (PEG-only gels), (2) with RGDS (persistently-presented RGDS gels), and (3) with RGDS for removal on Day 10 (photocleaved RGDS gels). Upon complete polymerization, cell-gel sheets were transferred to chondrogenic media supplemented with 5 ng/mL TGF-β_1 [DMEM with high glucose, ITS + premix (6.25 μg/mL bovine insulin, 6.25 μg/mL transferrin, 6.25 μg/mL selenous acid, 5.33 μg/mL linoleic acid, 1.25 μg/mL bovine serum albumin), 100 nM dexamethasone, 50 μg/mL ascorbic acid 2-phosphate, 100 μg/mL sodium pyruvate, 100 μg/mL penicillin-streptomycin, 1 μg/mL amphotericin B]. The media was refreshed after 30 mins, and media-swollen cell-gel disks (0.25-mm thick and 5-mm diameter) were cut and transferred to a 48-well plate with fresh chondrogenic media supplemented with TGF-β_1. Media was refreshed twice per week throughout culture.

To remove RGDS from the gels on Day 10, half of the RGD-containing gels were transferred to Phenol-red-free DMEM and exposed to UV light under sterile conditions

(365 nm at 10 mW/cm^2 for 20 minutes per side). These gels were subsequently transferred back to fresh chondrogenic media supplemented with TGF-β_1.

Cell-gel constructs were removed from culture at various time points to analyze DNA content, glycosaminoglycan (GAG) production, CD105 expression and collagen type II (COLII) production to establish hMSC chondrogenesis, and $\alpha_v\beta_3$ integrin expression for cell-RGD interaction (Day 0, 4, 7, 14, 17, and 21). For DNA and GAG analysis, the constructs were digested in a papain solution overnight at 60^{o}C. The amount of double-stranded DNA in these digestion solutions was analyzed using a PicoGreen Assay (Pierce), and viability was calculated by normalization of DNA production to Day 0 DNA production for each experimental condition. The same digestion solutions were analyzed with the dimethylmethylene blue (DMMB) assay (*S9*) for the amount of GAG deposition, and total GAG production was quantified for each time point and experimental condition. For CD105 expression, COLII production, and integrin expression, cell-gel constructs were fixed and cryosectioned at 40 μm for immunostaining. Sections were either stained (i) dually for expression of CD105 and COLII production or (ii) for expression of the $\alpha_v\beta_3$ integrin as described elsewhere (*S10*) and mounted with a Prolong Gold anti-fade reagent with DAPI (Invitrogen). All samples were imaged with an inverted epi-fluorescence microscope (Nikon TE2000S) in brightfield, DAPI, FITC, and TRITC, and at least 3 images were taken per sample per early and late time point (Day 4 and Day 21) with a 10x, 20x, and 40x objective and analyzed for staining. Using Matlab, background intensity was established in each fluorescent image using a round mask that was twice the pixel size of an individual cell

and was subtracted (i.e., uniform background subtraction); the contrast subsequently was uniformly adjusted across all images. To establish the percentage of cells differentiated into chondrocytes, 10x magnification images in DAPI, FITC, and TRITC were false-colored to aid in visualization of positively-stained cells and analyzed: cells producing COLII (chondrocytes) and cells strongly expressing CD105 (hMSCs) were counted, divided by the total number of cells stained with DAPI, and multiplied by 100%. To examine the production of COLII or expression of CD105 by individual cells, 40x magnification images were merged (BF, DAPI, FITC, and TRITC) and examined. To establish the percentage of cells expressing the integrin $\alpha_v\beta_3$, 20x magnification images in DAPI and FITC were analyzed: cells producing $\alpha_v\beta_3$ were counted, divided by the total number of cells stained with DAPI, and multiplied by 100%. To examine the expression of $\alpha_v\beta_3$ by individual cells, 20x magnification images were merged (BF, DAPI, and FITC) and examined.

Statistics

All data collected are presented as mean ± standard error of three or more samples. A Student's t-test was used to compare data sets using p values of 0.05 or less to determine statistical significance.

Supplemental online text

S1 - Light absorbance and attenuation in photodegradable hydrogels

Light absorbance by the photodegradable crosslinker was examined using a UV-visible spectrophotometer (UV-vis, Lambda 40 UV/Vis Spectrometer, Perkin Elmer, $8x10^{-5}$ M Compound 1 in DI water). Compound 1 absorbs strongly in the UV and visible region due to the photolabile moiety, as shown in Fig. S1, and this absorbance decreases slightly as the photolabile moiety is cleaved and subsequently photobleached (Novacure, EFOS, 100W mercury arc lamp with bandpass filters, liquid-filled light guide, and collimating lens, 10 mW/cm^2 365nm, 1 h; lamp system used for all studies unless otherwise noted).

This light absorbance leads to light attenuation within a photodegradable gel that is specific to the wavelength of light used for irradiation. Using the Beer-Lambert Law, the light intensity (I) at specific distance within the gel (d) can be calculated by

$$I = I_o \exp(-2.3\varepsilon dC)$$

where C is the a photolabile group concentration, ε molar absorptivity of the photolabile group at the wavelength of the incident light, and I_o is the incident light intensity (*S7*). With the molar absorptivity of the photodegradable crosslinker at any UV or visible light wavelength, the light attenuation for a particular crosslinker composition, sample thickness, and light wavelength can be calculated and thus exploited (i) to bulk degrade optically thin gels and (ii) to surface erode optically thick gels.

S2 - Resolution of gel erosion

This photolithographic technique can be used to create features of any size down to the resolution of the photomask printer (≤10 μm). Smaller features can be created with focused light, where feature size will simply be based on the diffraction limit of light for the wavelength used for degradation. Assuming a Gaussian laser beam with diameter D and a depth of focus L, the smallest feature size possible at a given numerical aperature (NA) is related to the wavelength of light and m

$$D_{FWHM} = \frac{2}{\pi}\frac{\lambda}{NA}\sqrt{\frac{\ln 2}{2m}} \qquad L_{FWHM} = \frac{2}{\pi}\frac{\lambda}{NA}\sqrt{2^{1/m}-1}.$$

In single photon photolysis, m=1 and degradation occurs at l=365nm, so D=137nm and L=232nm. This represents an unprecedented level of spatial control over hydrogel scaffold structure.

S3 - Additional three-dimensional patterning of photodegradable hydrogels to create 3D features within a gel

To illustrate the range of feature sizes that can be created with LSM patterning, 50 μm long cylinders of varying diameter were patterned (50, 25, 10, and 5 μm) with a two-photon confocal LSM (740 nm), as shown in Fig. S2A with brightfield and a top down confocal fluorescence slice with marked cross-sections. In addition to two-photon patterning, single-photon patterning within these photodegradable hydrogels is possible with a 405 nm laser; here, 5 triangles of varying size were scanned every 20 μm within a gel with a 405 nm single-photon laser to create a pyramid (Fig. S2B; 30 mW laser, 20x

objective NA ~ 0.75, laser power = 25%, scan speed setting = 7, cumulative scan time to create 3D feature = 34 s). With the single-photon 405 nm patterning, some pattern transfer from lower tiers can be seen in fluorescent images due to superposition of the out-of-focus regions of the write-beam.

S4 - Photolabile peptide gel synthesis, patterning, and release

To create photolabile biofunctional tether hydrogels with tunable chemical properties, the photolabile RGDS tether macromer (Compound 2) was polymerized into a non-degradable PEG hydrogel in PBS for 5 minutes between glass slides separated by a spacer (10 mM Compound 2, 10 wt% PEG diacrylate (PEGDA, M_n~4600 g/mol), 0.1 M AP, 0.05 M TEMED, 0.25-mm thick). Upon complete polymerization, gel disks were cut (0.25-mm thick and 5-mm diameter) and placed in PBS, which was refreshed. For 3D patterning samples, peptide gels were similarly created with photolabile peptide except that a small amount of fluorescently labeled photolabile peptide was added to the monomer solution (9.7 mM and 0.3 mM, respectively), and gel squares were cut (0.5-mm x 10 mm x 10 mm).

The photolabile peptide gel squares were patterned in 3D with a single-photon confocal LSM (405nm laser, laser power=25%, scan speed setting=6 or 7). Rows of three-dimensional 100 μm long cylinders with removed RGD were thus created with varying diameter (50, 25, and 10 μm). Regions without RGD were patterned, where the peptide-containing gel fluoresces green and cylinders with the peptide removed are dark (Fig. S3A).

For bulk release studies, gels were transferred to Phenol-red-free DMEM to simulate photocleavage under cell culture conditions. To photocleave the peptide and follow its release from the gel, gel disks were placed in plastic UV-vis cuvettes (1.5-mL Diposable cuvettes, Plastibrand) containing DMEM (1.25 mL) and exposed to UV light for varying time intervals (365 nm at 10 mW/cm^2, 5-minute exposure intervals separated by arbitrary amounts of time, 4 h, 1.5 h, and 0.5 h). The release of peptide from the gel was followed using a UV-vis, analyzing the change in absorbance at 340nm where the cleaved photolabile group that is attached to the peptide strongly absorbs. After these exposure intervals, samples were flood exposed to cleave any remaining peptide and determine the total peptide loaded in the gel (365 nm at 10 mW/cm^2 for 30 min, diffusion time of 1 day). Peptide release is represented as the fraction of peptide released from the gel, mass of peptide released at any time point (M_t) normalized to mass of total peptide loaded (M_∞) (Fig. S3B). Released peptide diffuses out of the gel in minutes.

S5 - Viability and spreading of hMSCs encapsulated in photodegradable gels

Photodegradable gels with encapsulated hMSCs were irradiated for 8 minutes per side to bulk degrade the gel (365 nm at 10 mW/cm^2). Cells were checked for viability with and without degradation (LIVE/DEAD Viability/Cytotoxicity Kit, Invitrogen). Cell viability was unaffected by the gel degradation (Fig. S4, Zeiss LSM 5 Pascal, Achroplan 10x NA 0.3W), comparing gels with and without degradation 4 days after light exposure.

S6 - hMSC viability and GAG production in non-degradable gels with photoreleasable RGDS

hMSC viability (Fig. 3C) is low in the PEG-only hydrogel for two reasons: (i) lack of cell adhesion to the PEG-based microenvironment without RGDS or ECM molecules and (ii) lack of cell-cell contact due to the low cell seeding density used to limit cell-cell contact and only test cell-material interactions. While RGDS can be added to the microenvironment to increase hMSC viability, a higher cell seeding density could also increase cell viability within the PEG-only gel. With the extreme disparity between viability in the PEG-only and RGDS-containing gels, GAG normalized to cell number or DNA is misleading, as the low viability makes GAG production appear large in PEG-only gels when it is not. Thus, total GAG production was presented in the manuscript text. For comparison, GAG normalized to DNA is presented here for the persistent and photoremoved RGDS gels, which have similar cell viability. An increase in GAG production is observed with photoremoval of RGDS (Fig. S5), consistent with Fig. 3C in the manuscript. The concentration of GAG appears to slightly decrease on Day 17, which is likely due to cell-remodeling of the secreted matrix via enzyme production (*S11*), although not a statistically-significant decrease from Day 14.

Supporting references

S1. Y. R. Zhao *et al.*, *Journal of The American Chemical Society* **126**, 4653 (Apr 14, 2004).
S2. M. Alvarez *et al.*, *Adv. Mater.* **20**, 4563 (Dec, 2008).
S3. W. C. Chan, P. D. White, Eds., *Fmoc Solid Phase Peptide Synthesis*, (Oxford University Press, Inc., New York, 2000), pp. 346.
S4. D. Li, D. L. Elbert, *J. Pept. Res.* **60**, 300 (Nov, 2002).

S5. R. P. Sebra, A. M. Kasko, K. S. Anseth, C. N. Bowman, *Sens. Actuator B-Chem.* **119**, 127 (Nov 24, 2006).
S6. R. J. Young, P. A. Lovell, *Introduction to polymers*. (Chapman & Hall, London, U. K., ed. 2nd, 1991), pp. 443.
S7. G. Odian, *Principles of polymerization*. (John Wiley & Sons, Inc., Hoboken, New Jersey, ed. 4th, 2004), pp. 812.
S8. S. J. Bryant, K. S. Anseth, in *Scaffolding in Tissue Engineering,* P. X. Ma, J. Elisseeff, Eds. (Marcel Dekker, Inc., 2005).
S9. R. W. Farndale, D. J. Buttle, A. J. Barrett, *Biochimica Et Biophysica Acta* **883**, 173 (Sep 4, 1986).
S10. C. N. Salinas, K. S. Anseth, *Biomaterials* **29**, 2370 (2008).
S11. A. M. DeLise, L. Fischer, R. S. Tuan, *Osteoarthritis Cartilage* **8**, 309 (Sep, 2000).

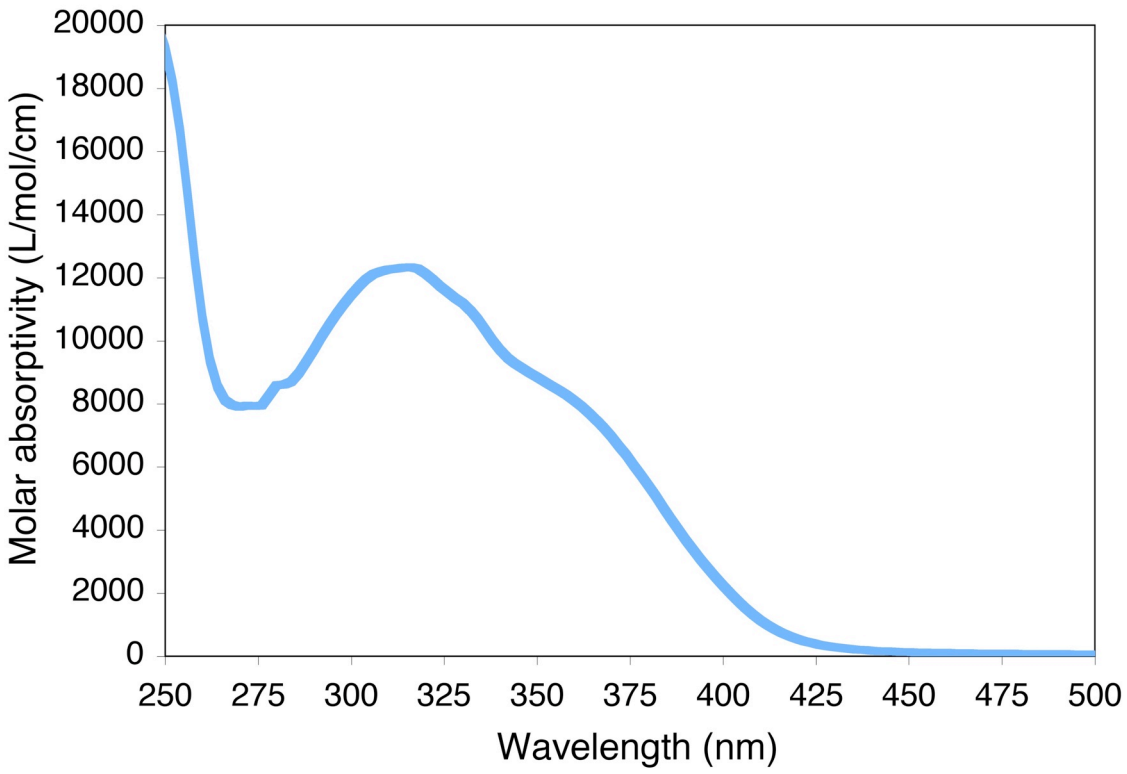

Figure S1. Photodegradable crosslinker light absorbance. Compound 1 and gels comprised of it absorb light strongly in the UV and visible regions, especially at readily-available light source wavelengths (ε_{365nm} = 7600 $Lmol^{-1}cm^{-1}$ and ε_{405nm} = 1640 $Lmol^{-1}cm^{-1}$).

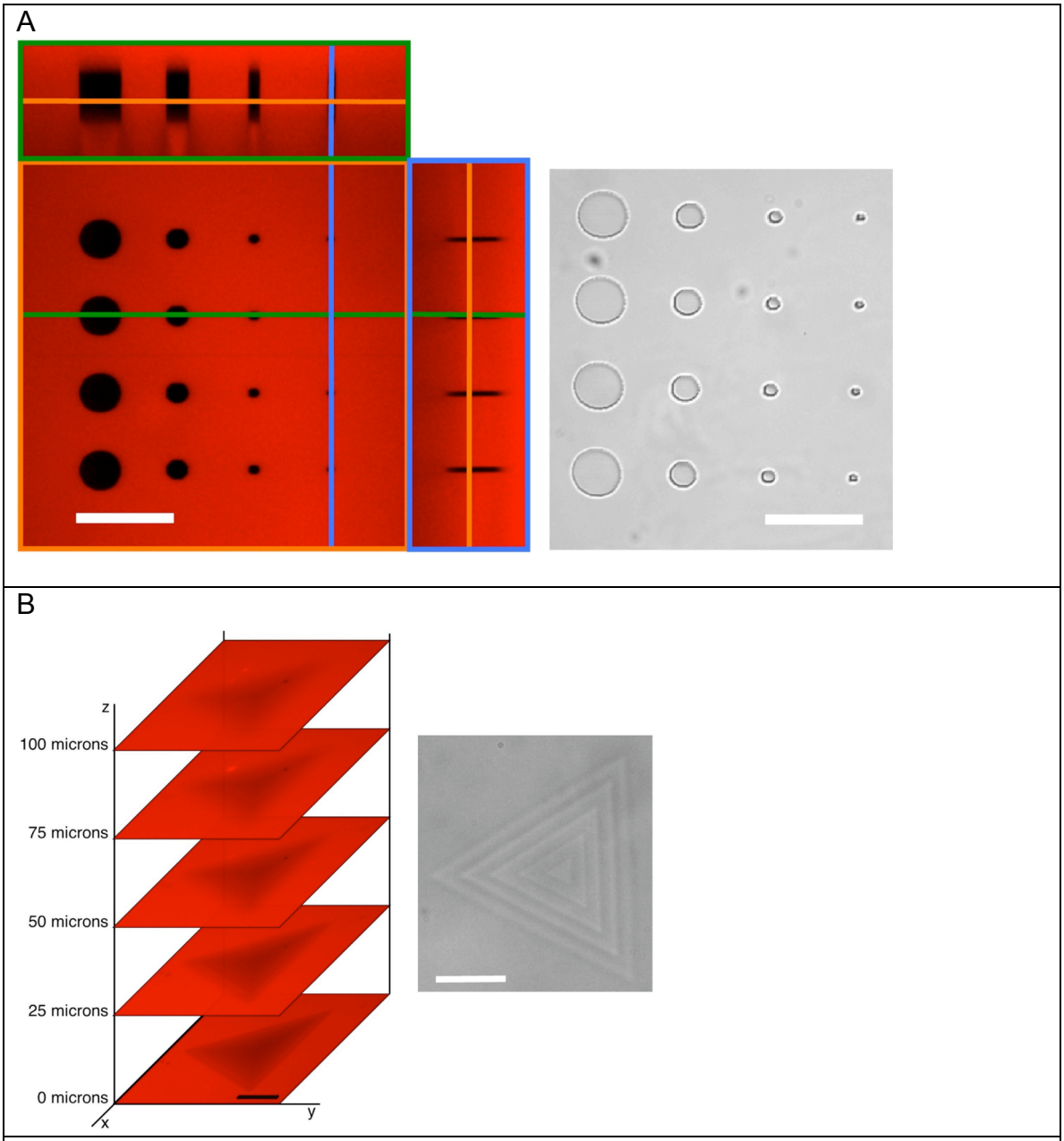

Figure S2. Photodegradable hydrogel 3D patterning. (A) Confocal LSM slice (left) with marked cross-sections of varying diameter columns patterned within a gel using a two-photon LSM (740nm, 50% power, and scan speed setting 8) and corresponding brightfield image (right). Pattern transfer is precise and quick for the facile creation on 3D features of varying size within a gel. **(B)** Confocal LSM stack (left) and brightfield image (right) of pyramid composed of stacked triangles of varying size that were patterned within a photodegradable gel using a single-photon LSM (405nm laser, 25% power, and scan speed setting 7). Scale bars, 100 μm.

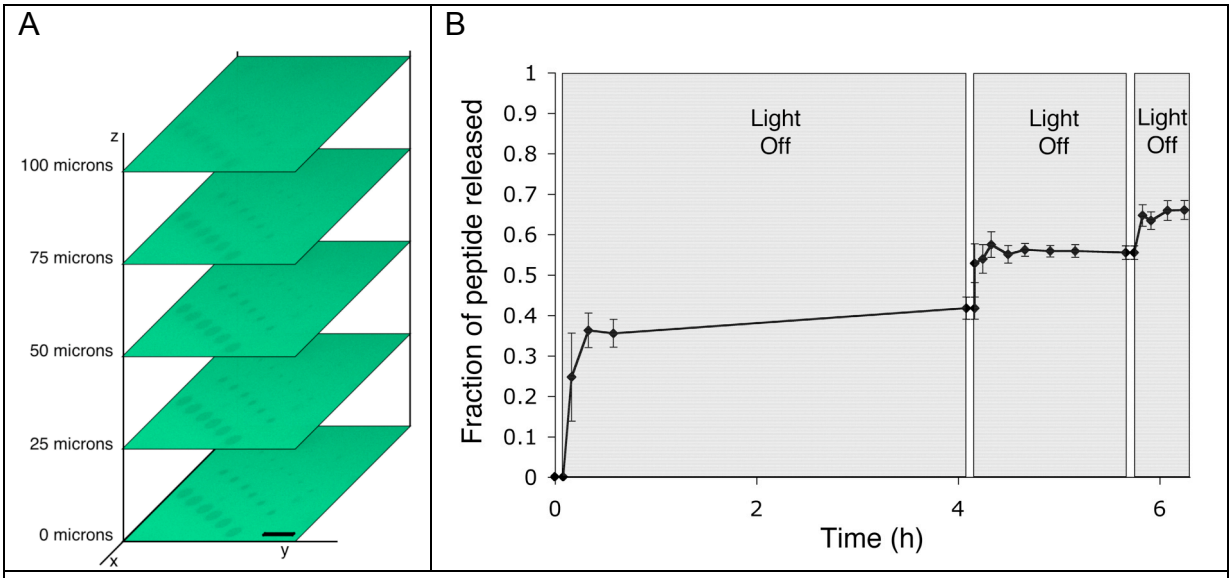

Figure S3. Photolabile peptide gel patterning and release. **(A)** Three-dimensional chemical features were created within an initially homogeneous gel using a single-photon LSM where shapes of varying size are scanned within the gel. RGDS is removed from the photolabile biofunctional gel in columns of varying diameter (approximately 50, 25, and 10 μm) and 100 μm in depth with a 405nm laser. The phototlabile peptide sequence, labeled with carboxyfluorescein for visualization, is photocleaved and released from the gel, creating dark columns with removed RGDS. **(B)** Release of the photodegradable peptide RGDS from a gel was controlled temporally with light exposure (5-minute exposure increments, 365 nm at 10 mW/cm^2, shuttered for arbitrary intervals). The photolabile group is cleaved, releasing RGDS into the solution followed by RGDS diffusion out of the hydrogel, which was monitored with a UV-vis spectrophotometer. Scale bars, 100 μm.

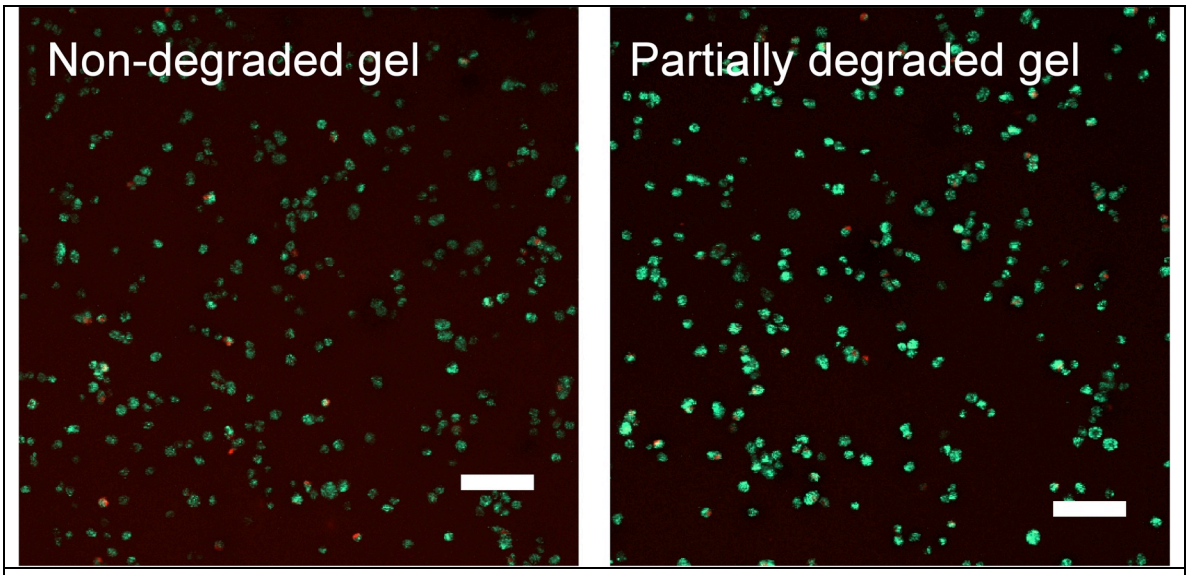

Figure S4. Cell viability in photodegradable hydrogels. Encapsulated hMSC viability is unaffected by partial degradation of the photodegradable hydrogel (right, 365 nm at 10 mW/cm^2, 8 min) as compared to hMSCs in non-degraded photodegradable hydrogels (left), where the gel is labeled with rhodamine for visualization (red background), live cells are green, and dead cells are red (Day 4 in 3D culture). These viable cells indicate that the hydrogel degradation products and irradiation conditions are relatively benign to these cells. Scale bars,100 μm.

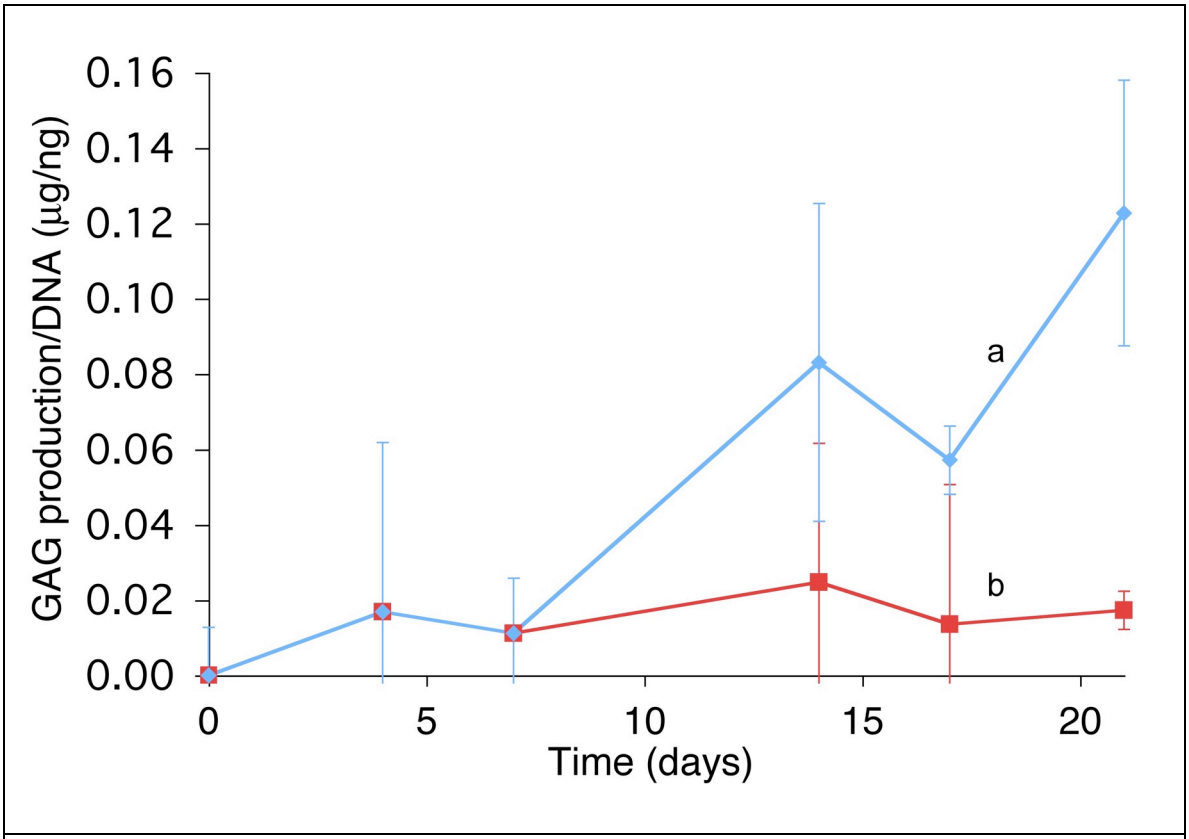

Figure S5. Normalized GAG production of encapsulated hMSCs. Persistent RGDS presentation decreases hMSC chondrogenic differentiation as compared to gels with RGDS photocleaved on Day 10. (a) RGDS photolytic removal increases GAG production normalized to DNA over (b) persistently presented RGDS by Day 21, indicating further hMSC chondrogenesis, where normalization eliminates any effect of cell number on GAG production.